Journal of Applied Fluid Mechanics, Vol. 9, No. 1, pp. 311-319, 2016.
Available online at www.jafmonline.net, ISSN 1735-3572, EISSN 1735-3645.
DOI: 10.18869/acadpub.jafm.68.224.22903

A Numerical Simulation on MHD Mixed Convection in a Lid-driven Cavity with Corner Heaters

A. Malleswaran[1] and S. Sivasankaran[2†]

[1]*KS Rangasamy College of Technology, Tiruchengode 637 215, India*
[2]*Institute of Mathematical Sciences, University of Malaya, Kuala Lumpur 50603, Malaysia*

†*Corresponding Author Email: sd.siva@yahoo.com*

(Received April 12, 2014; accepted January 7, 2015)

ABSTRACT

A numerical investigation on mixed convection in a lid-driven square cavity has been performed in the presence of the uniform magnetic field. From the left-bottom corner of the cavity, three different lengths of heater are varied along bottom and left walls simultaneously. The finite volume method is employed to solve the governing equations. It is observed that the heater length in the x-direction is more effective than that of in the y-direction on the heat transfer and on the flow pattern. The magnetic field affects the average heat transfer rate more on vertical heaters than on the horizontal heaters.

Keywords: Mixed convection; Magnetic field; Lid-driven cavity; Corner heating.

1. INTRODUCTION

Mixed convection is a combined result of two heat transfer mechanisms forced convection and natural convection and plays an important role in engineering, technology, and industries (Srivastava and Singh 2010, Bahlaoui *et al*. 2011). Guo and Sharif (2004) performed an analysis on mixed convection in a rectangular cavity. They found that the heat affected region becomes larger on increasing the length of the heat source and the temperature variation around the heat source is restricted in the free convection mode. Sharif (2007) explained the mixed convection in a shallow rectangular cavity for various Richardson numbers. It is found that the average Nusselt number increases more rapidly for Ri = 10 with the cavity inclination. Ji *et al.* (2007) studied the transient mixed convection in a lid-driven enclosure. It is observed that the temperature field shows weak fluctuating behavior at early times in the middle and upper portions of the cavity.

Bhuvaneswari *et al*. (2011) numerically studied the mixed convection flow, heat and mass transfer with Soret effect in a two-sided lid-driven square cavity. They found that heat and mass transfer rates decrease with the increase in the Richardson number. Oztop and Abu-Nada (2008) performed a numerical analysis on free convection in a partially heated rectangular enclosure filled with nanofluids. It is obtained that the heater location affects the flow pattern and the temperature distributions. Sivakumar *et al.* (2010) investigated mixed convection in a lid-driven cavity with different lengths and locations of heater. It is observed that the heat transfer rate is boosted up when the location of heater is at top or middle on the left wall. Sivasankaran *et al*. (2010) numerically studied mixed convection heat transfer in a lid-driven cavity with sinusoidal temperature distributions on both vertical walls. It is observed that the heat transfer rate is increased as the Richardson number increases. Sivasankaran *et al*. (2011) examined the effects of discrete heating on natural convection in a rectangular porous enclosure with a heat-generating substance. They found that the heat transfer rates are high at both heaters for smaller heater length ratio.

The study, Magneto-hydrodynamics (MHD), involving the influence of magnetic field on heat transfer and fluid flow within the cavity has received a considerable attention in recent years. The reason is the widespread practical applications of MHD convection in the fields such as solar technologies, material manufacturing technology, electromagnetic casting, liquid-metal cooling of nuclear reactors and plasma confinement (Patra *et al*. 2014, Rudraiah *et al*. 2014). Chamkha (2002) studied the mixed convection in a square cavity in the presence of a magnetic field with internal heat generation. The average Nusselt number is decreased on increasing the strength of magnetic field. Sarris *et al*. (2005) performed a numerical

study on magneto-convection of an electrically conducting fluid in a laterally and volumetrically heated square cavity. Hossain *et al*. (2005) examined the combined buoyancy and thermo-capillary convection in an enclosure in the presence of the magnetic field. It is observed that the applied magnetic field resists the flow and retards the velocity field. Sivasankaran and Ho (2008) reported a numerical investigation on natural convection of water near its density maximum under a uniform magnetic field. The heat transfer rate increases according to the increase in the Rayleigh number and decreases with an increase in the Hartmann number. Sivasankaran *et al*. (2011), Sivasankaran *et al*. (2011) numerically examined convection in a square cavity in the presence of a uniform external magnetic field.

Heaters take place over a narrow segment of the vertical walls in many engineering applications. In such cases, the size and location of the heater(s) play an important role on the fluid flow and heat transfer mechanisms. Hence, determining the optimum heater size and their location becomes noteworthy for better utilization of such systems. In fact, the corner heating during the mixed convection in square cavities has not received much attention. Hence, a numerical investigation involving MHD convection with corner heating would be helpful to enrich the ideology in thermally enhanced design of systems. The main objective of this paper is to provide the valid, essential and application oriented knowledge about the effects of corner heating on MHD mixed convection in a lid-driven cavity.

2. MATHEMATICAL FORMULATION

The physical situation is depicted by a schematic diagram of a two-dimensional square cavity of length L in Figure 1. It is assumed that the flow is unsteady, laminar, incompressible, and two-dimensional. The velocity components u and v are, respectively, along x-direction and y-direction. Letting the lid of the cavity to move in its own plane with a constant speed U_0, a part of the surfaces along left and bottom walls is maintained at a constant temperature θ_h and the right sidewall is at a lower temperature θ_c such that $\theta_h > \theta_c$. In fact, from the left-bottom corner of the cavity, three different lengths of heater are simultaneously considered along the bottom and left walls. For every length of the heater considered partly along the left wall of the cavity, three different constant lengths of heater are varied along its bottom wall. Thus, nine distinct configurations of corner heating are under investigation to examine the heat transfer characteristics and the flow behavior. The top wall and the remaining surfaces that are not heated on both left vertical wall and bottom wall are insulated. The gravity acts in the downward direction. The cavity is filled with an electrically conducting fluid of low Prandtl number. A uniform magnetic field is applied in the horizontal direction with a constant magnitude B_0. The electric current J and the electromagnetic force F are defined by $J = \sigma_e (V \times B)$ and $F = \sigma_e (V \times B) \times B$, respectively. The induced magnetic field due to the motion of the electrically conducting fluid is very small compared to the applied magnetic field. Therefore the magnetic Reynolds number is too small and it is neglected. Further, the viscous dissipation and Joule heating are assumed to be negligible. The governing equations are described as follows:

$$\frac{\partial u}{\partial x} + \frac{\partial v}{\partial y} = 0 \tag{1}$$

$$\frac{\partial u}{\partial t} + u\frac{\partial u}{\partial x} + v\frac{\partial u}{\partial y} = -\frac{1}{\rho_0}\frac{\partial p}{\partial x} + \nu\left(\frac{\partial^2 u}{\partial x^2} + \frac{\partial^2 u}{\partial y^2}\right) \tag{2}$$

$$\frac{\partial v}{\partial t} + u\frac{\partial v}{\partial x} + v\frac{\partial v}{\partial y} = -\frac{1}{\rho_0}\frac{\partial p}{\partial y} + \nu\left(\frac{\partial^2 v}{\partial x^2} + \frac{\partial^2 v}{\partial y^2}\right) + g\beta(\theta - \theta_c) - \frac{\sigma_e B_0^2 v}{\rho_0} \tag{3}$$

$$\frac{\partial \theta}{\partial t} + u\frac{\partial \theta}{\partial x} + v\frac{\partial \theta}{\partial y} = \frac{k}{\rho_0 c_p}\left(\frac{\partial^2 \theta}{\partial x^2} + \frac{\partial^2 \theta}{\partial y^2}\right) \tag{4}$$

where θ is the temperature, ρ_o is the density, p is the pressure, k is the thermal conductivity, ν is the kinematic viscosity, c_p is the specific heat, g is the gravitational acceleration, and t is the time.

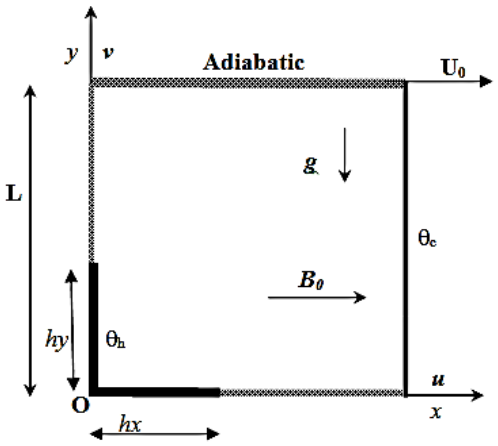

Fig. 1. Schematic diagram.

The appropriate initial and boundary conditions are expressed as follows:

For $t=0$: $u=v=0$, $\theta=0$ $0 \le (x, y) \le L$ (5)

For $t>0$:

$u = U_0; v = 0$ $\frac{\partial \theta}{\partial y} = 0$ $y = L$

$u = v = 0$ $\theta = \theta_h$ $y = 0, 0 \le x \le hx$ & $x = 0, 0 \le y \le hy$

$u = v = 0$ $\frac{\partial \theta}{\partial y} = 0$ $y = 0, hx < x \le L$

$u = v = 0$ $\theta = \theta_c$ $x = L$

$u = v = 0$ $\frac{\partial \theta}{\partial x} = 0$ $x = 0, hy < y \le L$

where $hx \,\&\, hy = L/4$, $2L/4$ and $3L/4$ denote the length of heaters along x-and y- directions, respectively. By varying heaters of constant length

from the left-bottom corner, on left and bottom sidewalls, there arise three different cases of corner heating. As a first case, the lengths of heater along bottom wall are varied as *L/4*, *L/2* and *3L/4* while a constant length *L/4* of heater along left vertical wall is considered. The remaining two cases are set up by changing the lengths along left wall as *L/2* and *3L/4* for the same heaters on bottom wall taken as in the earlier case.

The governing Eqns. (1) to (5) are transformed into dimensionless form by using the following non-dimensional variables $X=\frac{x}{L}$, $Y=\frac{y}{L}$, $U=\frac{u}{U_0}$, $V=\frac{v}{U_0}$, $Hx=\frac{hx}{L}$, $Hy=\frac{hy}{L}$, $T=\frac{\theta-\theta_c}{\theta_h-\theta_c}$, $\tau=\frac{tU_0}{L}$, $P=\frac{p}{\rho U_o^2}$, $\zeta=\omega L/U_0$ and $\Psi=\psi/LU_0$. After non-dimensionalization, the following set of equations is obtained in the form of vorticity-stream function formulation.

$$\frac{\partial\zeta}{\partial\tau}+U\frac{\partial\zeta}{\partial X}+V\frac{\partial\zeta}{\partial Y}=\frac{1}{\mathrm{Re}}\left(\frac{\partial^2\zeta}{\partial X^2}+\frac{\partial^2\zeta}{\partial Y^2}\right)+Ri\frac{\partial T}{\partial X}-\frac{Ha^2}{\mathrm{Re}}\frac{\partial V}{\partial X} \quad (6)$$

$$\nabla^2\Psi=-\zeta \quad (7)$$

$$\frac{\partial T}{\partial\tau}+U\frac{\partial T}{\partial X}+V\frac{\partial T}{\partial Y}=\frac{1}{\mathrm{Pr}\,\mathrm{Re}}\left(\frac{\partial^2 T}{\partial X^2}+\frac{\partial^2 T}{\partial Y^2}\right) \quad (8)$$

$$U=\frac{\partial\Psi}{\partial Y},\ V=-\frac{\partial\Psi}{\partial X}\ \text{and}\ \zeta=\frac{\partial V}{\partial X}-\frac{\partial U}{\partial Y} \quad (9)$$

The dimensionless parameters in the above equations (6) to (8) are defined as follows: $\mathrm{Ha}=B_0L\sqrt{\sigma_e/\mu}$, the Hartmann number, $Pr=\nu/\alpha$ (=0.054), the Prandtl number, $Re=U_0L/\nu$, the Reynolds number, $Ri=Gr/Re^2$, where $Gr=g\beta\Delta TL^3/\nu^2$, the Grashof number.

The initial and boundary conditions are expressed in dimensionless form as follows:

For $\tau=0$:

$$U=V=\zeta=\Psi=0 \quad T=0 \quad 0\le(X,Y)\le 1$$

For $\tau>0$:

$$U=1, V=\Psi=0,\ \zeta=-\frac{\partial^2\Psi}{\partial Y^2},\ \frac{\partial T}{\partial Y}=0 \quad Y=1$$

$$U=V=\Psi=0,\ \zeta=-\frac{\partial^2\Psi}{\partial Y^2},\ T=1 \quad Y=0,\ 0\le X\le Hx$$

$$U=V=\Psi=0,\ \zeta=-\frac{\partial^2\Psi}{\partial X^2},\ T=1 \quad X=0,\ 0\le Y\le Hy$$

$$U=V=\Psi=0,\ \zeta=-\frac{\partial^2\Psi}{\partial X^2},\ \frac{\partial T}{\partial X}=0 \quad X=0,\ Hy\le Y\le 1$$

$$U=V=\Psi=0,\ \zeta=-\frac{\partial^2\Psi}{\partial Y^2},\ \frac{\partial T}{\partial Y}=0 \quad Y=0,\ Hx\le X\le 1$$

$$U=V=\Psi=0,\ \zeta=-\frac{\partial^2\Psi}{\partial X^2},\ T=0 \quad X=1 \quad (10)$$

The local Nusselt numbers for heating surfaces along bottom and vertical walls are respectively given by $Nu_x=\left(-\frac{\partial T}{\partial Y}\right)_{Y=0}$, $Nu_y=\left(-\frac{\partial T}{\partial X}\right)_{X=0}$ whereas for cold wall, it is obtained from $Nu_c=\left(-\frac{\partial T}{\partial X}\right)_{X=1}$.

The average Nusselt number along the cold wall is computed by $\overline{Nu_c}=\int_0^1 Nu_c\,dY$.

The non-dimensional equations (6)–(9) are solved by finite volume method. The detailed method of solution can be found in Sivasankaran *et al.* (2011). The validation of the present computational code is verified with convective flow in lid-driven cavities (Sharif 2007, Iwatsu *et al.* 1993) and shown in Table 1. The obtained results show a good agreement with the available results.

Table 1 Comparison of average Nusselt number for lid-driven cavity

Re	*Gr*	Average Nusselt number		
		Present work	Sharif (2007)	Iwatsu *et al.* (1993)
400	10^2	4.08	4.05	3.84
	10^4	3.84	3.82	3.62
	10^6	1.10	1.17	1.22
1000	10^2	6.48	6.55	6.33
	10^4	6.47	6.50	6.29
	10^6	1.66	1.81	1.77

3. RESULTS AND DISCUSSION

The lengths of the corner heater along horizontal and vertical directions are taken as 0.25, 0.5, and 0.75. For a fixed Grashof number $Gr=10^4$ and the variations of Reynolds number (*Re*) from 10 to 10^3, the range of Richardson number is set as $0.01\le Ri\le 100$. The values of the Hartmann number are taken to be 0, 25 and 100. The value of Prandtl number is chosen as 0.054 corresponding to the liquid metal.

3.1 Effects of Various Lengths of Heater

Figures 2(a)-(c) illustrate the isotherms for different lengths of the heater which are varied from left-bottom corner of the cavity along the left sidewall and bottom wall for various Richardson numbers and Ha=25. As a first case, keeping the length of heater along the left sidewall as *Hy*=0.25, the lengths of heater along bottom wall are varied from 0.25 to 0.75; see Figures 2(a). The second and third cases occur for the vertical lengths of heater 0.5 and 0.75, respectively, while the lengths of heater along bottom wall are varied as earlier. Obviously, for all the three cases, an enhanced temperature distribution is observed around the heated regions along both directions. Due to sharp temperature gradients near the left wall, a strong thermal boundary layer is formed along the heaters when

forced convection dominates. Further, the temperature distributions show curl like distribution due to strong convection.

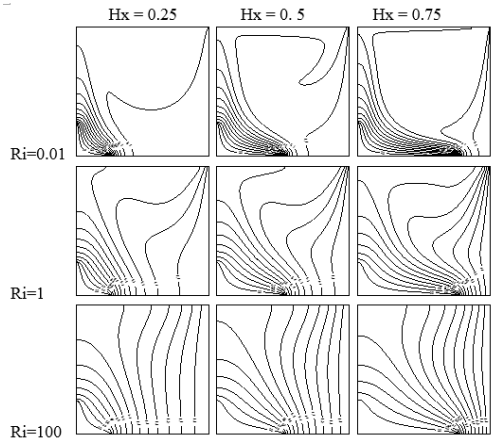

(a) Hy = 0.25

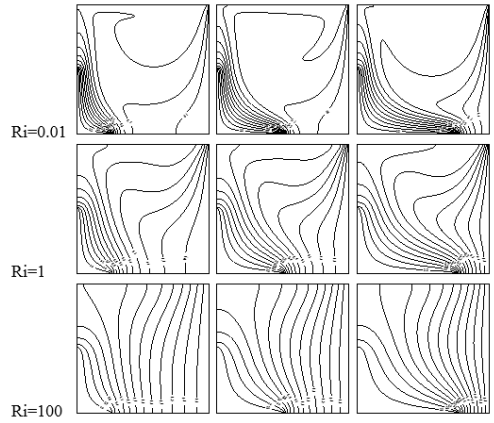

(b) Hy = 0.5

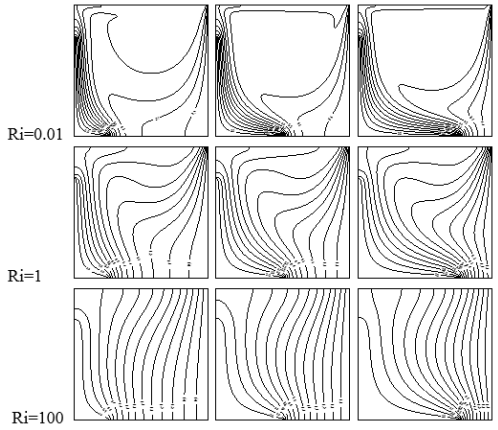

(c) Hy = 0.75

Fig. 2(a-c). Isotherms of different heating regions on both x and y directions with different Richardson numbers with Ha = 25.

The horizontal heated layer remains closer to the bottom wall of the cavity. When the lengths of heater along the bottom wall are 0.5 and 0.75, it seems that a thin boundary layer appears at the right-top corner of the cavity. For further increase in the lengths of heater along left sidewall, it is interesting to see that the formation of the thin boundary layer on the cold wall gradually increases; see Figures 2(b-c). Though the lengths of heater are equally considered along both directions, temperature distribution is getting better according to the increase in lengths of the heater. In general, the heat distribution is better when the vertical lengths of heater are increased than that of the increase in the bottom lengths of heater. In the mixed convection regime, the formation of boundary layers along heaters gradually decreases. In the buoyancy-driven convection mode, i. e. for *Ri*=100, temperature gradients occur uniformly throughout the cavity and boundary layers on either side of the vertical walls disappear. The strong thermal boundary layer near the heaters along both directions and the thin boundary layer near cold wall formed in the forced convection regime disappear in the buoyancy-driven convection mode. In a differentially heated cavity, the thermal boundary layer is formed along the both hot and cold wall. Hence, it is confirmed that corner heating ideology is entirely different from differentially heated cavity.

The fluid flow of the varied lengths of heater along left and bottom walls for various Richardson numbers is shown in Figures 3(a)-(c). In all the three cases of variations in length of heater along both directions, the flow field consists of single clockwise cell. Since the cavity is heated partly along both vertically and horizontally, the heated particles near bottom wall are also raised adjacent to the heater on left sidewall and fall along the opposite cold wall. The clustered streamlines near the top wall indicate that steep velocity gradients occur near the top wall. Hence, the center of the cell is near the top wall for all the Richardson numbers. The cell is slightly elongated in all the cases of length variation while natural convection dominates. Particularly, the speed of the flow is almost uniform throughout the cavity and the increase in the lengths of heater shows no significant change in the flow field.

Figure 4(a-b) depicts the influence of vertical lengths of heater on heat transfer rate while *Hx* is kept constant at 0.5. It can be understood that the heat transfer is enhanced well at *Hy*=0.75 and it becomes low at *Hy*=0.25 in the dominance of forced convection. But, in the case of natural convection, high heat transfer occurs at *Hy*=0.5 and heat transfer is observed to be low for *Hy*=0.75. On the other hand, these results turn out opposite when the horizontal lengths of heater are varied while *Hy*=0.5. i.e. highest local Nusselt number occurs at *Hx*=0.5 when Ri = 0.01 and the length *Hx*=0.5 results the lowest local Nusselt number for *Ri*=100. These can be witnessed in Figures 4(c-d).

The overall heat transfer rate of cold wall for various lengths of heater along horizontal and vertical directions against the Richardson numbers with Ha=25 is exemplified in Figures 5(a)-(c). It can be observed that the average heat transfer rate is strictly increased when the horizontal lengths of heater is increased. Particularly, for all vertical lengths *Hy*, the average Nusselt number gets its highest value for the maximum horizontal length *Hx*=0.75 compared with the others. Moreover, it

can be verified that overall heat transfer rate is firmly increased while increasing the vertical lengths of heater. Generally, it can be concluded that the increase in lengths of heater along either of the directions result in the increase of overall heat transfer rate. Also, it is observed that the heater length in the *x*-direction is more effective than that of in the *y*-direction on the heat transfer and on the flow pattern. The average heat transfer decreases when the Richardson number is increased.

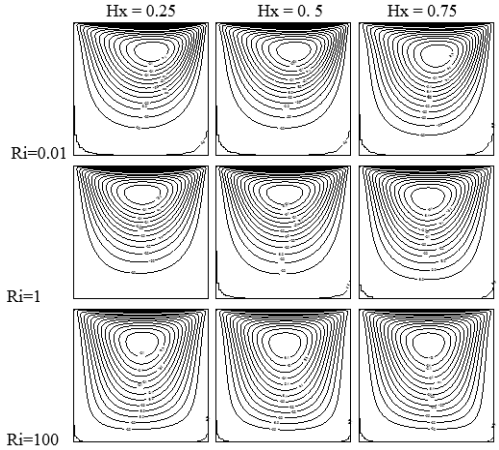

(a) Hy = 0.25

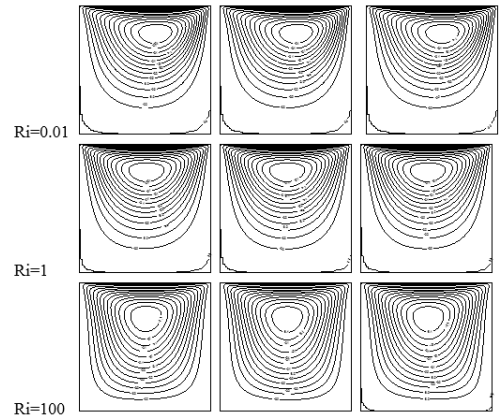

(b) Hy = 0.5

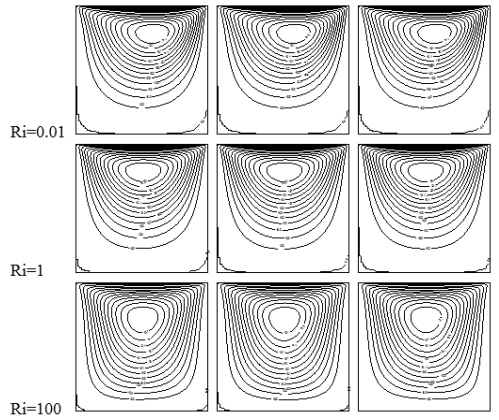

(c) Hy = 0.75

Fig. 3(a-c). Streamlines of different heating regions on both x and y directions with different Richardson numbers with Ha = 25.

However, the overall heat transfer is better and independent of the variations in the Richardson numbers for the maximum heater length 0.75 along both directions.

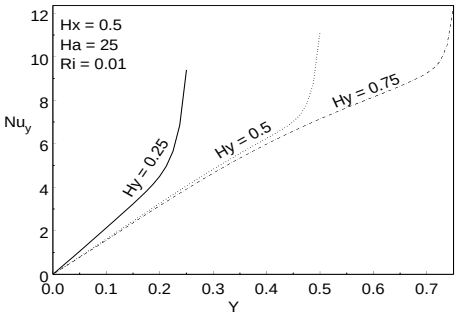

(a)

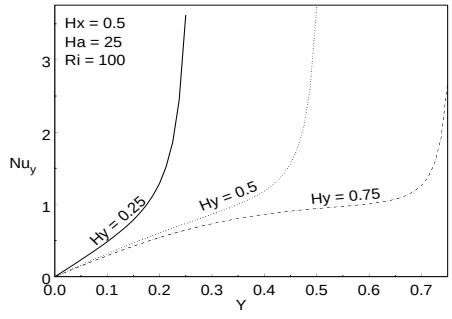

(b)

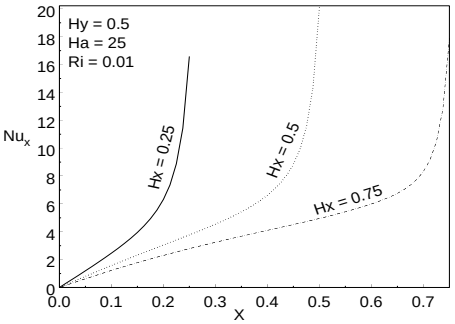

(c)

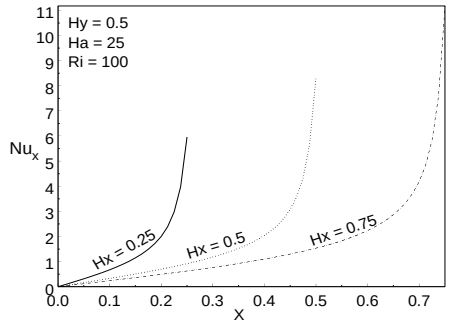

(d)

Fig. 4 (a-d). Local Nusselt numbers for different heating regions and for different Richardson numbers with Ha = 25.

Figures 6(a)-(c) exhibit the influence of various Hartmann numbers on temperature distribution and fluid flow for Ri=0.01 and Ri=100 when the lengths of heater are considered equally on both vertical and horizontal directions. Either Ha=0 or Ha=25, the temperature distribution is enhanced through convection mode due to the shear force generated by the moving top wall at Ri=0.01. For these values of the Hartmann number, no

remarkable changes are noticed in the isotherms. This reveals the fact that still forced convection dominates the heat transfer mechanism and weak magnetic field does not create any impact on the heat distribution remarkably. On the other hand, if the Hartmann number is increased to 100, the isotherms seem to be straightened out, i.e., the energy transportation is changed to conduction mode. Since the convective heat distribution is affected by the strong magnetic field Ha=100, the thermal boundary layers near hot and cold walls vanish. During the forced convection dominance, the flow is described by a single clockwise rotating cell in the entire cavity at Ha=0 and 25. The speed of the fluid flow decreases owing to the increase in the magnetic field. A resistive force due to strong magnetic field controls the speed of the fluid particles and results in the suppression of fluid flow.

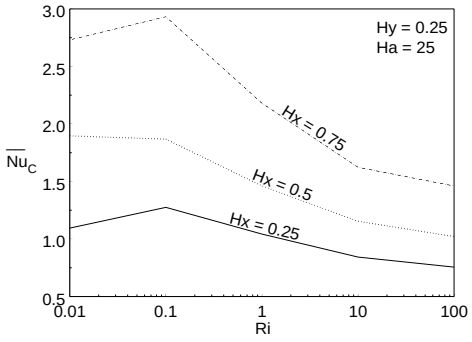

(a)

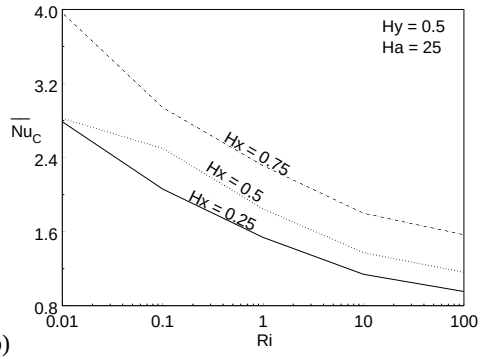

(b)

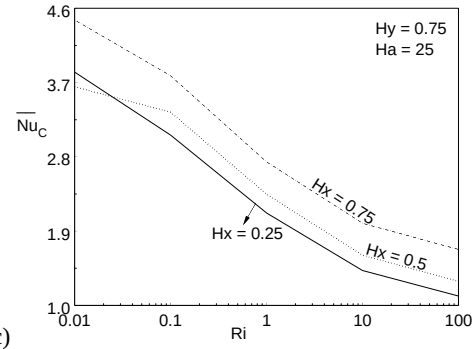

(c)

Fig. 5(a-c). Average Nusselt number of cold wall for various Richardson numbers and different lengths of heating region along both x and y directions.

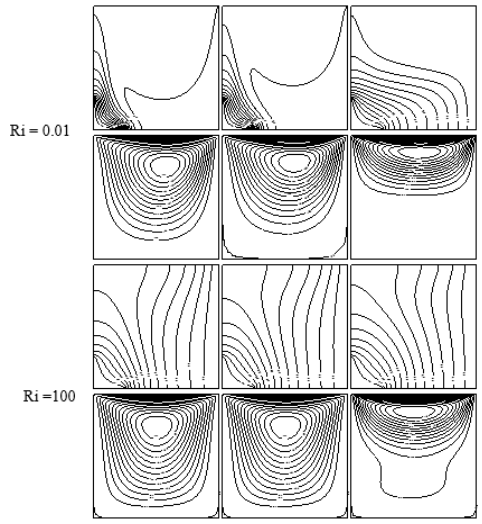

(a) Hx = 0.25; Hy = 0.25

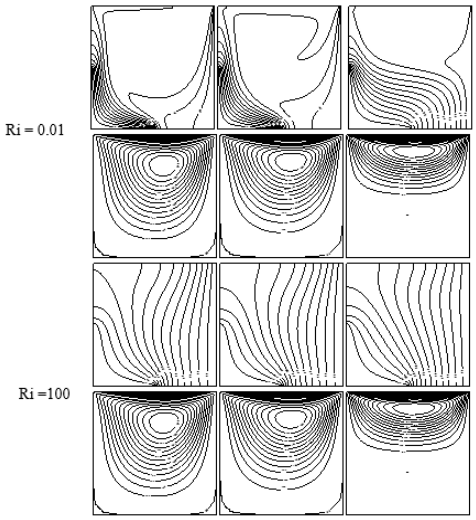

(b) Hx = 0.5; Hy = 0.5

Ha=0 Ha=25 Ha=100

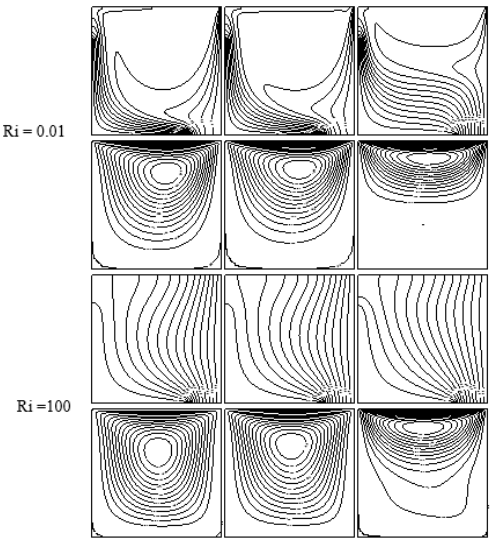

(c) Hx = 0.75; Hy = 0.75

Fig. 6. Isotherms and streamlines of different Hartmann numbers and Richardson numbers.

3.2 Effects of the Hartmann Number

On the other hand, when the buoyancy-driven convection dominates, i.e. at Ri=100, the isotherms are almost parallel to the vertical walls, indicating that most of the heat transfer process is carried out by conduction. No other notable change is observed in the heat transfer though the Hartmann numbers are varied for the considered lengths of heater. But, noteworthy changes can be viewed in the fluid flow. For all the lengths of heater, when Ha=0 or 25, a similar behavior in the flow is sighted. But, on imposing a strong magnetic field such as Ha=100, the core region of the eddy is inhibited very close to the top wall of the cavity. Meanwhile, the vortex is elongated vertically for both the lengths 0.25 and 0.75 of the heater along both directions. When the length of heater is *Hx*=*Hy*=0.5, there exists consistency in the flow speed and so is in the flow pattern. The flow becomes broadly stagnated in the lower part of the cavity. It is observed that the convective motion is totally inhibited with the increase of the Hartmann numbers. Further, it is proved that the fluid flow is independent on the lengths of heater since effect of magnetic field is significant in either of the cases, the forced convection and the natural convection.

The changes on overall heat transfer rate along cold wall are shown in Figures 7(a)-(e) for different lengths of heater and the Hartmann numbers. As a general behavior, it is observed that the average Nusselt numbers are decreased when the Hartmann number is increased. When *Hx*=*Hy*=0.25, the effects for low Hartmann numbers such as 0 and 25 vanish up to Ri=0.1 and a sudden increase in the average heat transfer rate is shown with the increase in the Richardson numbers. Thereafter, it is gradually decreased while the Richardson numbers are increased; see Figures 7(a-c). From forced convection regime to mixed convection regime, the average heat transfer rate is independent of the magnetic field and is not even affected a little for the Hartmann numbers 0, 25 and 100 when *Hy*=0.25 and *Hx*= 0.75. It is seen that the overall heat transfer rate is reduced as the Hartmann number increases when *Hy*=0.75 and *Hx*= 0.25. The average heat transfer rate is very low for Ha=100 and the lengths of heater on bottom and left walls are 0.25.

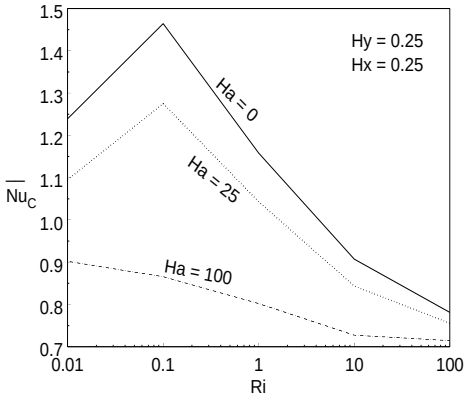

(a)

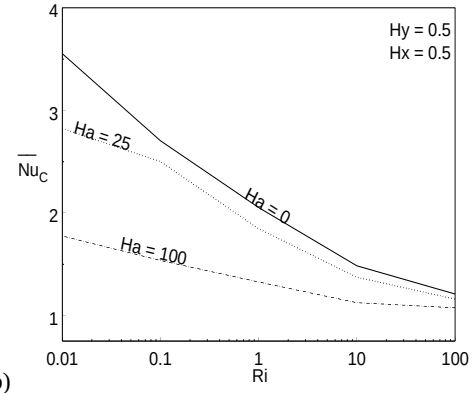

(b)

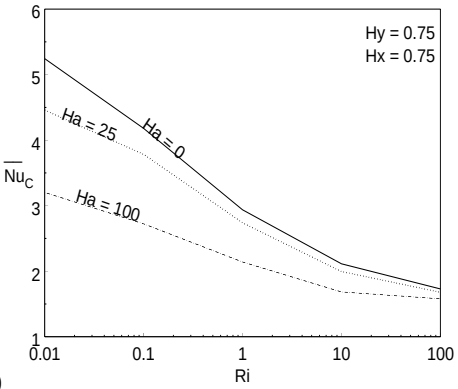

(c)

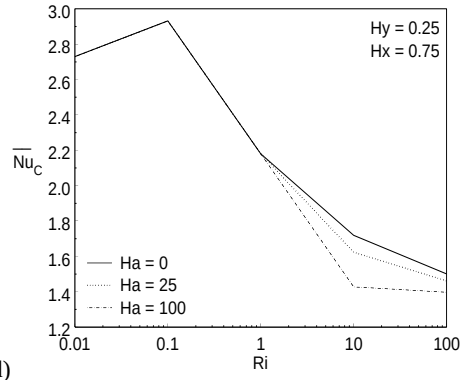

(d)

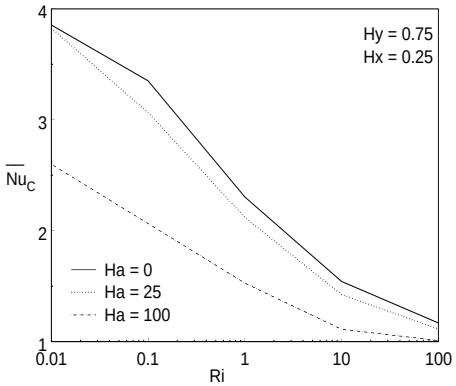

(e)

Fig. 7. Average Nusselt number of cold wall versus Richardson numbers for different lengths of heating region along both x and y directions and Hartmann numbers.

4. CONCLUSION

The effects of corner heating on mixed convection under the influence of a uniform magnetic field in a lid-driven square cavity are discussed. The following conclusions are drawn.

1. When the vertical (horizontal) length of the heater is kept constant and the horizontal (vertical) length is varied, the average heat transfer is higher for the maximum horizontal (vertical) heater length *Hx*= 0.75 (*Hy*= 0.75). It is observed that the heater length in the *x*-direction is more effective than that of in the *y*-direction on heat transfer.

2. For the equal lengths of heater considered simultaneously along bottom and left walls, it is shown that the overall heat transfer rate is enhanced (on increasing the heater size) for the maximum length *Hx*=*Hy*=0.75 of heater.

3. The applied magnetic field affects the overall heat transfer more on vertical heaters than along the horizontal heaters. Generally, the average heat transfer decreases on increasing the Richardson number. The overall heat transfer is better at forced convection mode than at free convection mode.

4. Cavity with corner heaters is completely different from differentially heated cavity in which the thermal boundary layer occurs near both hot and cold walls whereas no such boundary layer exist in the cavity with corner heaters at forced convection mode.

ACKNOWLEDGEMENTS

The authors would like to thank the University of Malaya for the financial support through the grants: RG216-12AFR and RP011B-13AFR.

REFERENCES

Srivastava, N. and A. K. Singh (2010). Mixed Convection in a Composite System Bounded by Vertical Walls. *J. Applied Fluid Mech.* 3(2), 65-75.

Bahlaoui, A., A. Raji, M. Hasnaoui, C. Ouardi, M. Naïmi and T. Makayssi (2011). Height Partition Effect on Combined Mixed Convection and Surface Radiation in a Vented Rectangular Cavity. *J. Applied Fluid Mech.* 4(1), 89-96.

Guo, G. and M. A. R. Sharif (2004). Mixed convection in rectangular cavities at various aspect ratios with moving isothermal sidewalls and constant flux heat source on the bottom wall. *Int. J. Therm. Sci.* 43, 465–475.

Sharif, M. A. R. (2007). Laminar mixed convection in shallow inclined driven cavities with hot moving lid on top and cooled from bottom. *Appl. Therm. Engg*. 27, 1036–1042.

Ji, T. H., S. Y. Kim and J. M. Hyun (2007). Transient mixed convection in an enclosure driven by a sliding lid. *Heat. Mass. Trans.* 43, 629–638.

Bhuvaneswari, M., S. Sivasankaran and Y. J. Kim (2011). Numerical study on double diffusive mixed convection with a Soret effect in a two-sided lid-driven cavity. *Numer. Heat. Trans. A.* 59, 543–560.

Oztop, H. F. and E. Abu-Nada (2008). Numerical study of natural convection in partially heated rectangular enclosures filled with nanofluids. *Int. J. Heat and Fluid Flow* 29, 1326–1336.

Sivakumar, V., S. Sivasankaran, P. Prakash and J. Lee (2010). Effect of heating location and size on mixed convection in lid-driven cavities. *Computers Math. Appl* 59, 3053–3065.

Sivasankaran, S., V. Sivakumar and P. Prakash (2010). Numerical study on mixed convection in a lid-driven cavity with non-uniform heating on both sidewalls. *Int. J. Heat. Mass. Trans.* 53, 4304–4315.

Sivasankaran, S., Y. Do and M. Sankar (2011). Effect of discrete heating on natural convection in a rectangular porous enclosure. *Transp. Porous Med.* 86, 291–311.

Patra, R., S. Das and R. Nath Jana (2014). Radiation Effect on MHD Fully Developed Mixed Convection in a Vertical Channel with Asymmetric Heating, *J. Applied Fluid Mech*. 7(3), 503-512.

Rudraiah, N., B. M. Rajaprakash and Nagaraju (2014). Non-Linear Oberbeck Convection in Chiral Fluid through a Vertical Permeable Channel in the Presence of a Transverse Magnetic Field. *J. Applied Fluid Mech*. 7(1), 35-41.

Chamkha, A. J. (2002). Hydromagnetic combined convection flow in a vertical lid-driven cavity with internal heat generation or absorption. *Numer. Heat. Trans. A*, 41, 529–546.

Sarris, I. E., S. C. Kakarantzas, A. P. Grecos and N.S. Vlachos (2005). MHD natural convection in a laterally and volumetrically heated square cavity. *Int. J. Heat Mass Trans.* 48, 3443–3453.

Hossain, M. A., M. Z. Hafizb and D. A. S. Rees (2005), Buoyancy and thermocapillary driven convection flow of an electrically conducting fluid in an enclosure with heat generation. *Int. J. Therm. Sci. 44, 676–684.*

Sivasankaran, S. and C. J. Ho (2008). Effect of temperature dependent properties on MHD convection of water near its density maximum

in a square cavity. *Int. J. Therm. Sci.* 47, 1184–1194.

Sivasankaran, S., A. Malleswaran, J. Lee and P. Sundar, (2011). Hydro-magnetic combined convection in a lid-driven cavity with sinusoidal boundary conditions on both sidewalls. *Int. J. Heat. Mass. Trans.* 54, 512–525.

Sivasankaran, S., M. Bhuvaneswari, Y. J. Kim, C. J. Ho and K. L. Pan (2011). Numerical study on magneto-convection of cold water in an open cavity with variable fluid properties. *Int. J. Heat and Fluid Flow* 32, 932–942.

Iwatsu, R., J. M. Hyun and K. Kuwahara (1993). Mixed convection in a driven cavity with a stable vertical temperature gradient, *Int. J. Heat. Mass. Trans.* 36, 1601–1608.